

Fourier Series-Based Approximation of Time-Varying Parameters Using the Ensemble Kalman Filter

Anna Fitzpatrick, Molly Folino, Andrea Arnold*

Department of Mathematical Sciences, Worcester Polytechnic Institute, Worcester, MA, USA

*corresponding author: anarnold@wpi.edu

Abstract

In this work, we propose a Fourier series-based approximation method using ensemble Kalman filtering to estimate time-varying parameters in deterministic dynamical systems. We demonstrate the capability of this approach in estimating both sinusoidal and polynomial forcing parameters in a mass-spring system. Results emphasize the importance of the choice of frequencies in the approximation model terms on the corresponding time-varying parameter estimates.

Keywords: inverse problems; parameter estimation; time-varying parameters; approximation model; data assimilation.

1 Introduction

The goal of this research is to address time-varying parameter estimation in deterministic dynamical systems when there is no known (or available) model governing the evolution of the unknown parameter(s). In particular, we assume an ordinary differential equation (ODE) model of the form

$$\frac{dx}{dt} = f(t, x, \theta), \quad x(0) = x_0 \quad (1)$$

where $t \in \mathbb{R}$ denotes time, $x = x(t) \in \mathbb{R}^d$ is the vector of model states, $\theta = \theta(t) \in \mathbb{R}^p$ is the time-varying parameter vector of interest, and the mapping $f : \mathbb{R} \times \mathbb{R}^d \times \mathbb{R}^p \rightarrow \mathbb{R}^d$ is generally nonlinear. Given (potentially partial) observations of the system states $x(t)$ at some discrete times t_j , our goal is to estimate $\theta(t)$. Time-varying parameter estimation problems of this type arise in a variety of application areas, including biology [1, 2] and electric power systems [3, 4].

In this work, we propose an approximation method based on Fourier series, where we represent $\theta(t)$ as a linear combination of a finite number of sine and cosine functions and estimate the unknown coefficients using ensemble Kalman filtering. Previous work has utilized Fourier series for linear function approximation in reinforcement learning [5] and for estimating periodic time-varying parameters in the setting of adaptive control [6–8], where $\theta(t)$ is assumed to be periodic with a known period. Our goal is to approximate more general $\theta(t)$, including periodic parameters for which the period is unknown or is not contained within the time interval of observed data.

The use of data assimilation approaches such as ensemble Kalman filtering allows for sequential updating of the coefficient values along with the system states as new data arrives, without relying on the full time series of data in advance. Ensemble-based methods also provide a natural measure

of uncertainty in the resulting parameter estimate, generally taken as ± 2 standard deviations around the mean. Previous studies have used nonlinear filtering to estimate the coefficients of piecewise functional representations of periodic time-varying parameters [1, 9] or in conjunction with time-varying parameter tracking schemes [2, 4, 10–13].

In numerical examples utilizing a forced mass-spring system, we first establish the ability of the proposed method to estimate a periodic forcing parameter with known period, comparing the results when we have partial vs. full system observations. We then analyze the effects of modifying the approximation models to include more terms with differing frequencies to accommodate cases when the period of $\theta(t)$ is unknown. We further demonstrate the capability of the proposed method in estimating polynomial parameters which are not periodic over the time interval of observed data, and show that the resulting parameter approximation models can be utilized in making reasonable predictions of the system dynamics.

The paper is organized as follows. Section 2 reviews ensemble Kalman filtering and describes the proposed Fourier series-based approximation method for time-varying parameters. Section 3 details the results of the numerical experiments, and Section 4 gives a discussion and conclusions.

2 Methods

In this section, we briefly review ensemble Kalman filtering for combined state and parameter estimation and describe the Fourier series-based approximation method proposed in this work.

2.1 Ensemble Kalman Filtering

The ensemble Kalman filter (EnKF) is a Bayesian filtering algorithm that uses ensemble statistics within the framework of the classic Kalman filter to track unknown model variables given observed time series data [14, 15]. The incorporation of a statistical sample, which represents an underlying probability distribution of the unknowns conditioned on the available data, accommodates the use of nonlinear and possibly non-Gaussian models. The EnKF can be utilized to estimate unobserved (or unobservable) states of the model, as well as unknown parameters through use of an augmented system

$$\frac{dz}{dt} = \begin{bmatrix} \frac{dx}{dt} \\ \frac{d\theta}{dt} \end{bmatrix}, \quad z(0) = \begin{bmatrix} x(0) \\ \theta(0) \end{bmatrix} \in \mathbb{R}^{d+p} \quad (2)$$

where dx/dt gives the system dynamics, defined as in (1), and $d\theta/dt$ describes the dynamics of the parameters [16, 17]. In particular, $d\theta/dt = 0$ in the case of constant parameters.

Given a discrete sample of the model states and parameters at time j ,

$$\mathcal{S}_j = \{(x_j^1, \theta_j^1), \dots, (x_j^N, \theta_j^N)\} \quad (3)$$

the EnKF works as a two-step updating scheme: first, each pair of states and parameters is predicted at time $j + 1$ using the evolution model in (2); then, the augmented vectors are corrected using the Kalman filter observation updating equation, which incorporates the observed data at time $j + 1$. This process is illustrated in Figure 1, and the steps of the algorithm for combined state and constant parameter estimation are outlined in Algorithm 1.

Note that in the prediction step of Algorithm 1, the function F in line 4 denotes the solution to (1) at time $j + 1$ and the parameter values are not updated (since $d\theta/dt = 0$ for constant parameters). In the observation update, y_{j+1} in line 7 denotes the vector of observed model

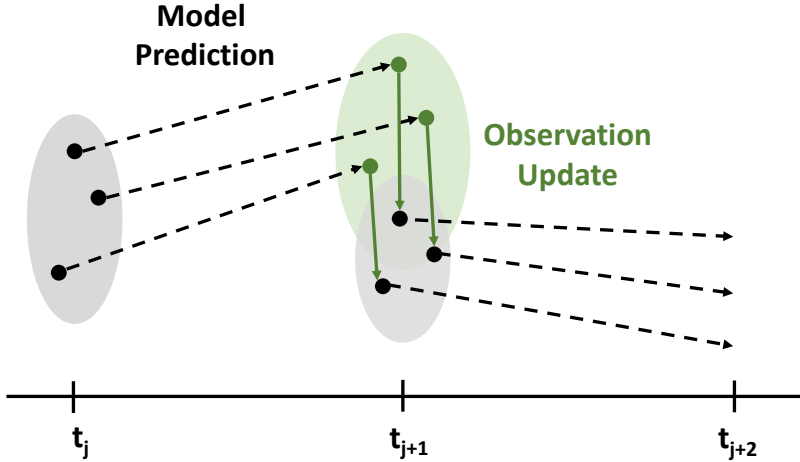


Figure 1: Illustration of the EnKF two-step updating scheme. In the prediction step, the ensemble members (represented as black circles, with sample variance in gray) at time j are each propagated forward (shown with black arrows) to time $j + 1$ by solving the model in (2). In the observation update, the ensemble predictions (green circles) are corrected (green arrows) using the observed system data at time $j + 1$. The process then continues using the corrected sample at time $j + 1$ (black circles).

states, with dimension $m \leq d$, which is perturbed to avoid too low a covariance in the resulting sample [15]. The updating equation in line 8 corrects the joint predicted sample for each n using the Kalman gain matrix K_{j+1} and the difference between the perturbed observation y_{j+1}^n and predicted observation $G(z_{j+1}^n)$, where G is the observation model. For linear observations, $G(z_{j+1}^n) = P z_{j+1}^n$ where $P \in \mathbb{R}^{m \times (d+p)}$ is a projection matrix whose entries corresponding to observed states are 1 and entries corresponding to unobserved states and parameters are 0. The posterior ensemble statistics computed in lines 9 and 10 give the mean and covariance, respectively, of the resulting sample at time $j + 1$. The process repeats sequentially until all available data in the time series is assimilated. In this procedure, parameter values are artificially evolved with the aim of converging to a constant.

2.2 Fourier Series-Based Approximation of Time-Varying Parameters

While the EnKF algorithm reviewed in Section 2.1 is formulated for constant parameter estimation, our goal in this work is to estimate time-varying system parameters for which no evolution model is known (or available); i.e., we do not have a known form of $d\theta/dt$ for $\theta = \theta(t)$. To address this problem, we utilize a Fourier series-based approximation in which $\theta(t)$ is represented as a linear combination of sine and cosine functions with different frequencies.

Recall that the Q th order Fourier series of a univariate function $h(t)$ is given by

$$h(t) = \frac{a_0}{2} + \sum_{q=1}^Q \left(a_q \cos \left(\frac{2\pi q t}{P} \right) + b_q \sin \left(\frac{2\pi q t}{P} \right) \right) \quad (4)$$

where a_q and b_q are the expansion coefficients and P is the period. Note that if $h(t)$ is known, the

Algorithm 1: EnKF for Combined State and Constant Parameter Estimation

Input: Initial sample \mathcal{S}_0 drawn from prior distribution $\pi(x_0, \theta_0)$
Output: Posterior sample \mathcal{S}_T and corresponding ensemble statistics

```

1 Initialize time index  $j = 0$ 
2 while  $j < T$  do
3   /* Prediction Step */ 
4   for  $n = 1, \dots, N$  do
5      $x_{j+1}^n = F(x_j^n, \theta_j^n) + v_{j+1}^n, \quad v_{j+1}^n \sim \mathcal{N}(0, \mathbf{C})$ 
6      $z_{j+1}^n = [x_{j+1}^n; \theta_j^n]$ 
7   /* Observation Update */ 
8   for  $n = 1, \dots, N$  do
9      $y_{j+1}^n = y_{j+1} + w_{j+1}^n, \quad w_{j+1}^n \sim \mathcal{N}(0, \mathbf{D})$ 
10     $z_{j+1}^n = z_{j+1}^n + \mathbf{K}_{j+1}(y_{j+1}^n - G(z_{j+1}^n))$ 
11   /* Compute Posterior Ensemble Statistics */ 
12    $\bar{z}_{j+1}^n = \frac{1}{N} \sum_{n=1}^N z_{j+1}^n$ 
13    $\Gamma_{j+1} = \frac{1}{N-1} \sum_{n=1}^N (z_{j+1}^n - \bar{z}_{j+1}^n)(z_{j+1}^n - \bar{z}_{j+1}^n)^\top$ 
14   /* Update Time Index */ 
15    $j = j + 1$ 

```

coefficients a_q and b_q can be computed explicitly by

$$a_q = \frac{2}{P} \int_0^P h(t) \cos\left(\frac{2\pi qt}{P}\right) dt \quad (5)$$

$$b_q = \frac{2}{P} \int_0^P h(t) \sin\left(\frac{2\pi qt}{P}\right) dt \quad (6)$$

However, in using Fourier series for function approximation, it is often the case that $h(t)$ is unknown and these coefficients must be estimated [5, 6, 8].

Inspired by the Fourier series, we represent the unknown time-varying parameter $\theta(t)$ in this work as a linear combination of sine and cosine pairs, such that the estimate of $\theta(t)$ is given by

$$\theta_{\text{est}}(t) = \sum_{i=1}^M \left(a_i \sin(\omega_i t) + b_i \cos(\omega_i t) \right) \quad (7)$$

with coefficients a_i, b_i and fixed angular frequencies ω_i . For simplicity moving forward, we denote the $2M$ coefficients by $c_k, k = 1, \dots, 2M$. Our goal in approximating $\theta(t)$ is therefore to estimate the $2M$ coefficients c_k that provide the best fit between the model in (7) and the true time-varying parameter given the available system data. We utilize the EnKF algorithm described in the previous section to estimate these coefficients.

Note that for cases in which we do not assume a known period of $\theta(t)$, we choose different values of ω_i such that the sine and cosine pairs in the approximation model (7) have different frequencies; i.e., $\omega_i = 2\pi f_i$ with frequency f_i . Numerical results demonstrate the importance of choosing appropriate frequencies for these functions, in particular the impact of including high and low frequency terms in the approximation model on the resulting $\theta(t)$ estimate.

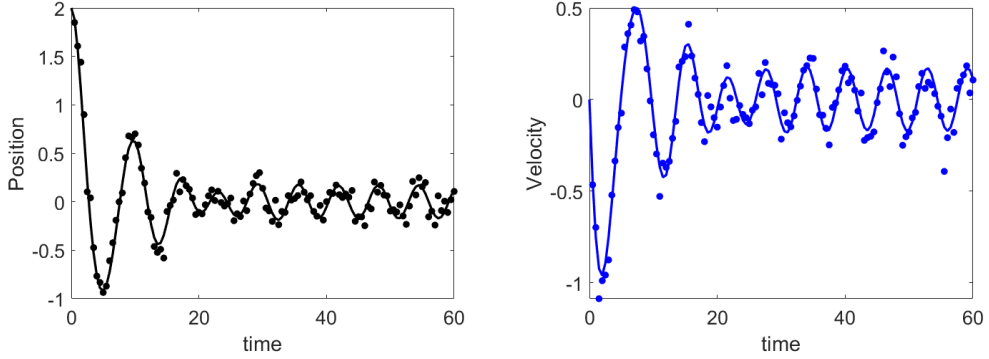


Figure 2: Position (left) and velocity (right) data generated from the forced mass-spring system (9) when $\theta(t) = \sin(t)$. On each plot, the solid line is the true solution to (9) and the circular markers show the noisy observations.

3 Numerical Results

In this section, we perform numerical experiments demonstrating the effectiveness of the proposed method under different scenarios in which $\theta(t)$ is a periodic parameter with a known period, an assumed to be unknown period, and when $\theta(t)$ is a polynomial function that is not periodic over the time interval of available data. Results were generated using MATLAB programming language.

We consider as an example a forced mass-spring system, classically modeled using the second-order ODE

$$mp'' + bp' + kp = \theta(t) \quad (8)$$

where $p = p(t)$ denotes the position (or displacement) of the mass at time t , $m > 0$ is the constant mass, $b > 0$ is the damping coefficient, and $k > 0$ is the spring constant [18]. Here $\theta(t)$ represents external forcing applied to the system, which we treat as our time-varying parameter of interest. Letting $v(t) = p'(t)$ denote the velocity of the mass, we can rewrite (8) as a first-order ODE system of the form

$$\frac{dx}{dt} = \begin{bmatrix} 0 & 1 \\ -\frac{k}{m} & -\frac{b}{m} \end{bmatrix} + \begin{bmatrix} 0 \\ \frac{\theta(t)}{m} \end{bmatrix} \quad (9)$$

where $x(t) = [p(t); v(t)] \in \mathbb{R}^2$ is the vector of model states. We assume that the constants m , b , and k are known, and our goal is to estimate $\theta(t)$ using the method described in Section 2.2.

To test the effectiveness of the proposed estimation method, we first generated synthetic data from the mass-spring system (9) using initial conditions $x(0) = [2; 0]$, fixed constants $m = 10$, $b = 3$, and $k = 5$, and different functional forms for $\theta(t)$. We solved the system (9) using MATLAB's built-in ODE solver `ode45` and recorded observations every 0.5 time units over the interval $[0, 60]$. Observations were then corrupted by Gaussian noise with zero mean and standard deviation 0.08. Figure 2 shows the generated data when $\theta(t) = \sin(t)$. A similar process was followed to generate data using the linear and cubic polynomial forcing parameters discussed in Section 3.3.

To initialize the EnKF, we set the sample size to $N = 1,000$ and drew the prior ensemble of state values from a multivariate Gaussian distribution with mean $[1; 1] \in \mathbb{R}^2$ and covariance matrix $(0.5)^2 I_2$, where I_2 denotes the 2×2 identity matrix. The prior ensemble of values for the unknown coefficients c_k were drawn uniformly over the interval $[-2, 12]$. Further, we assigned the model innovation covariance matrix (used in line 4 of Algorithm 1) to be $C = (0.02)^2 I_2$ and the observation covariance matrix (used in line 7 of Algorithm 1) to be $D = (0.08)^2$ for partial system

Coefficient	Position	Velocity	Position and Velocity
c_1	0.8390 ± 1.1648	0.9012 ± 1.0023	0.9575 ± 1.0087
c_2	-0.0249 ± 1.1862	-0.0247 ± 0.9057	0.0004 ± 0.9924
RMSE	0.1146	0.0717	0.0299

Table 1: Final coefficient estimates (mean \pm 2 standard deviations) and RMSE values to four decimal places for the approximation model $\theta_{\text{est}}(t) = c_1 \sin(t) + c_2 \cos(t)$ when estimating the forcing parameter $\theta(t) = \sin(t)$, observing data for only position, only velocity, and both position and velocity.

observations (i.e., observing only position or velocity) or $D = (0.08)^2 I_2$ for full system observations (i.e., observing both position and velocity) as detailed in the experiments that follow.

3.1 Partial vs. Full System Observations

We begin by utilizing a simple two-term series

$$\theta_{\text{est}}(t) = c_1 \sin(t) + c_2 \cos(t) \quad (10)$$

to approximate the true forcing parameter $\theta(t) = \sin(t)$, using the EnKF to estimate the coefficients c_1 and c_2 . In particular, we analyze the effects on the resulting coefficient estimates when the filter is given partial vs. full system observations; i.e., observations of only position (with velocity unobserved), only velocity (with position unobserved), and both position and velocity. Note that since the terms in the approximating series (10) have the same frequency as the true $\theta(t)$, an exact fit would correspond to $c_1 = 1$ and $c_2 = 0$.

Figure 3 shows the EnKF time series estimates (mean \pm 2 standard deviation curves) for the coefficients c_1 and c_2 along with the approximation $\theta_{\text{est}}(t)$ computed using the final coefficient mean estimates at time $t = 60$ in each case. Table 1 reports the final coefficient estimates (mean \pm 2 standard deviations) at time $t = 60$ and the corresponding root mean square error (RMSE) values, computed by

$$\text{RMSE} = \sqrt{\frac{\sum_{j=1}^T (\theta_{\text{est}}(t_j) - \theta(t_j))^2}{T}} \quad (11)$$

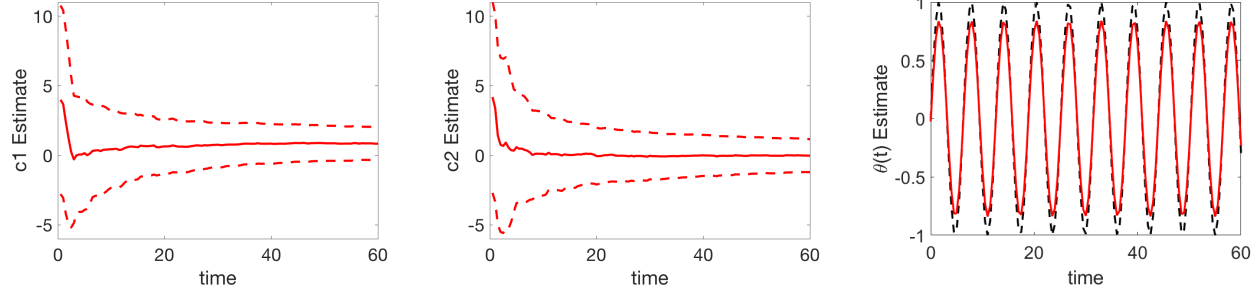
where T is the number of time points used in the discrete approximation, which here is the same as the number of observations.

As seen in Figure 3, in all three cases the coefficient estimates for c_1 and c_2 well converge to the constant values given in Table 1. When observing only position, the resulting approximation $\theta_{\text{est}}(t)$ has the same shape as the true $\theta(t) = \sin(t)$ but with smaller amplitude. When observing only velocity, the resulting approximation is slightly more accurate, with an amplitude closer to the true $\theta(t)$ and decreased RMSE. Observing both position and velocity data results in the most accurate approximation of the three, with the smallest RMSE and estimated coefficient values of $c_1 \approx 0.9575$ and $c_2 \approx 0.0004$. Noting this result, full system observations are used in the remaining numerical experiments.

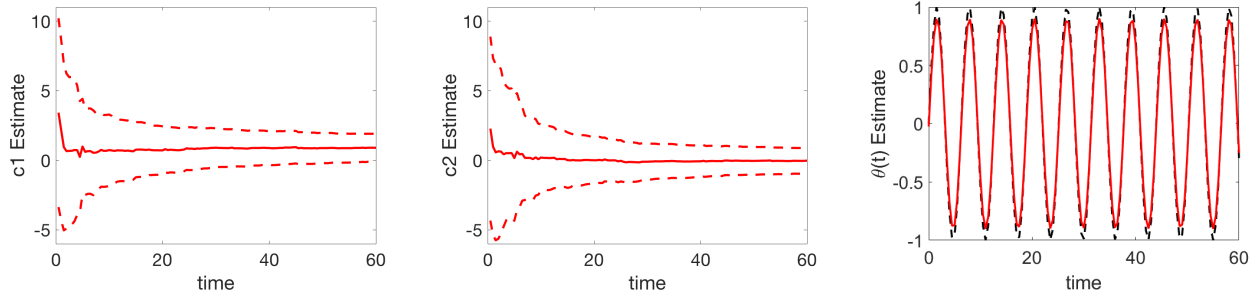
3.2 Approximation Models with Differing Frequency Terms

In the next set of numerical experiments, we assume that the true frequency of $\theta(t)$ is not known and expand upon the approximation model in (10) to include additional terms in the series with higher and lower frequencies. In particular, we assume observations of both position and velocity

Only Position Observed (Velocity Unobserved)



Only Velocity Observed (Position Unobserved)



Both Position and Velocity Observed

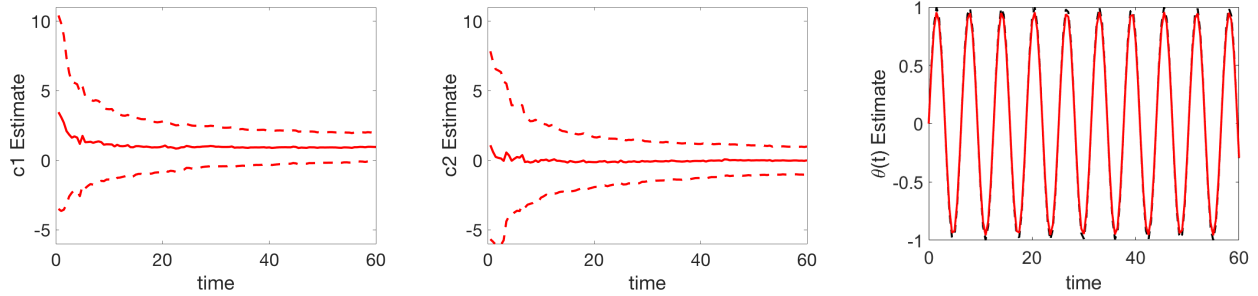


Figure 3: EnKF time series estimates for the coefficients c_1 and c_2 (left and middle columns) along with the approximation $\theta_{\text{est}}(t)$ in (10) computed using the final coefficient mean estimates (right column) when estimating the forcing parameter $\theta(t) = \sin(t)$, observing data for only position, only velocity, and both position and velocity. In each coefficient time series plot, the EnKF mean is shown in solid red with the ± 2 standard deviation curves shown in dashed red. In each approximation plot, $\theta_{\text{est}}(t)$ is shown in solid red and the true $\theta(t)$ is shown in dashed black.

are available and employ the following three approximation models for $\theta_{\text{est}}(t)$ (along with the names we will refer to them by) to again estimate $\theta(t) = \sin(t)$:

Low Frequency Series:

$$\begin{aligned}\theta_{\text{est}}(t) = & c_1 \sin(t) + c_2 \cos(t) + c_3 \sin(0.5t) + c_4 \cos(0.5t) + c_5 \sin(0.25t) + c_6 \cos(0.25t) \\ & + c_7 \sin(0.125t) + c_8 \cos(0.125t)\end{aligned}\quad (12)$$

High Frequency Series:

$$\begin{aligned}\theta_{\text{est}}(t) = & c_1 \sin(t) + c_2 \cos(t) + c_3 \sin(1.125t) + c_4 \cos(1.125t) + c_5 \sin(1.25t) + c_6 \cos(1.25t) \\ & + c_7 \sin(1.5t) + c_8 \cos(1.5t)\end{aligned}\quad (13)$$

Mixed Frequency Series:

$$\begin{aligned}\theta_{\text{est}}(t) = & c_1 \sin(t) + c_2 \cos(t) + c_3 \sin(1.5t) + c_4 \cos(1.5t) + c_5 \sin(0.5t) + c_6 \cos(0.5t) \\ & + c_7 \sin(1.75t) + c_8 \cos(1.75t) + c_9 \sin(0.25t) + c_{10} \cos(0.25t)\end{aligned}\quad (14)$$

Note that the approximation models in (12), (13), and (14) all include terms with the same frequency as $\theta(t)$ along with additional terms with frequencies that are multiplicative factors of this frequency (lower, higher, or mixed). In order to maintain balance between the higher and lower frequency terms considered, the Mixed Frequency Series (14) contains 10 terms, while the Low Frequency Series (12) and High Frequency Series (13) each contain 8 terms.

Figure 4 shows the resulting $\theta_{\text{est}}(t)$ time-varying parameter approximations computed using the final coefficient estimates in each case, and Table 2 gives the final coefficient estimates and corresponding RMSE values. As these results show, while all three models provide reasonable approximations to the true forcing parameter, the nonzero effects of the differing frequency terms lead to inaccuracies. This is particularly visible in Figure 4 around times 20 and 45 in each case, where there is a clear under-approximation of the true sine curve. The most accurate approximation in these experiments comes from using the Low Frequency Series (12).

3.3 Polynomial Parameter Estimation and Predicted System Dynamics

In this numerical experiment, we utilize the Fourier-series based approximation method to estimate polynomial forcing parameters, which we do not assume to be periodic over the time interval of observed data. More specifically, we estimate a linear forcing parameter with $\theta(t) = -0.07t + 2$ and a cubic forcing parameter with $\theta(t) = 0.0001(t - 25)^3 - 0.001t^2 + 3$. Hypothesizing that a linear combination of lower frequency terms will enable us to approximate time-varying parameters with non-oscillatory behavior, we introduce the following approximation model:

$$\begin{aligned}\theta_{\text{est}}(t) = & c_1 \sin(0.125t) + c_2 \cos(0.125t) + c_3 \sin(0.0625t) + c_4 \cos(0.0625t) + c_5 \sin(0.03125t) \\ & + c_6 \cos(0.03125t) + c_7 \sin(0.0156t) + c_8 \cos(0.0156t)\end{aligned}\quad (15)$$

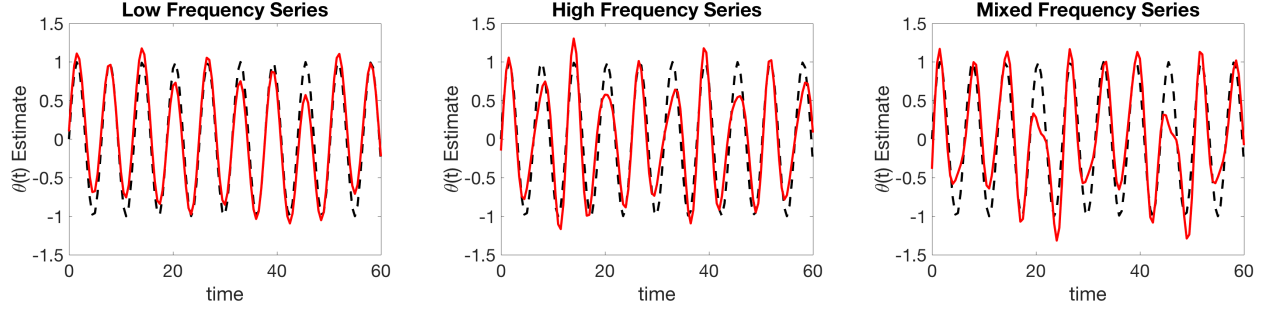


Figure 4: The approximation $\theta_{\text{est}}(t)$ computed using the final coefficient mean estimates for the Low Frequency Series (12) (left), High Frequency Series (13) (middle), and Mixed Frequency Series (14) (right) when estimating the forcing parameter $\theta(t) = \sin(t)$, observing data for both position and velocity. In each plot, $\theta_{\text{est}}(t)$ is shown in solid red and the true $\theta(t)$ is shown in dashed black.

Coefficient	Low Frequency	High Frequency	Mixed Frequency
c_1	0.9129 ± 1.0872	0.8572 ± 1.0761	0.8427 ± 1.0528
c_2	0.0387 ± 1.0582	0.0025 ± 1.0989	-0.0520 ± 1.0543
c_3	0.1333 ± 0.9095	0.0168 ± 1.1832	0.1364 ± 1.5758
c_4	0.0822 ± 0.9288	-0.0518 ± 1.1930	-0.1106 ± 1.4875
c_5	0.1082 ± 0.9649	-0.1065 ± 1.2349	0.0924 ± 0.8960
c_6	-0.0147 ± 0.9837	0.0266 ± 1.2859	0.0536 ± 0.8935
c_7	0.1420 ± 1.0229	0.2690 ± 1.5441	0.2288 ± 1.8645
c_8	-0.0070 ± 1.0257	-0.1255 ± 1.5327	-0.0816 ± 1.6903
c_9	—	—	0.1447 ± 0.9328
c_{10}	—	—	-0.1953 ± 1.0007
RMSE	0.1785	0.2442	0.2973

Table 2: Final coefficient estimates (mean \pm 2 standard deviations) and RMSE values to four decimal places for the Low Frequency Series (12), High Frequency Series (13), and Mixed Frequency Series (14) approximation models when estimating the forcing parameter $\theta(t) = \sin(t)$, observing data for both position and velocity.

The left column in Figure 5 shows the resulting $\theta_{\text{est}}(t)$ approximations computed using the final coefficient estimates in each case, which are given in Table 3 along with the corresponding RMSE values. These results show that, while there is some error in using the approximation model in (15), we are able to capture the overall trend of the parameter evolution in each case. Additionally, the middle and right columns in Figure 5 display the predicted mass-spring system states obtained by using the corresponding linear and cubic forcing parameter approximations in system (9) and solving with the same initial values used to generate the data. Despite the error in the parameter approximations, results demonstrate that we are still able to utilize these approximations to make reasonable predictions of the system dynamics.

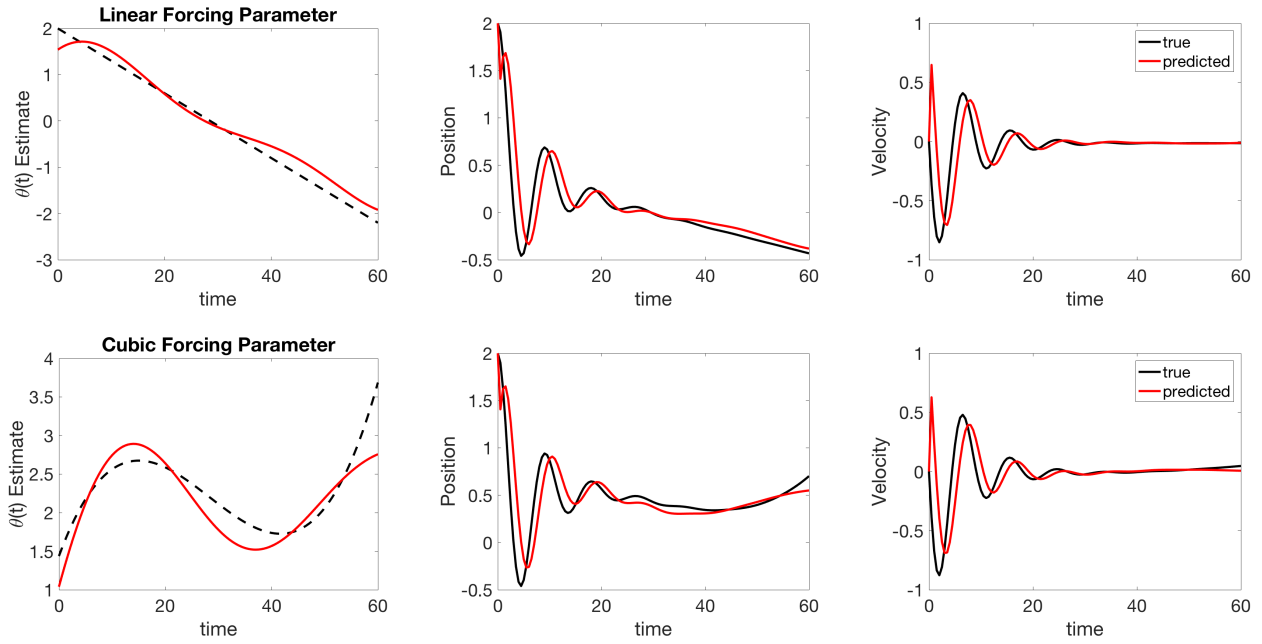


Figure 5: The approximation $\theta_{\text{est}}(t)$ (left) computed using the final coefficient mean estimates for model (15) when estimating the linear forcing parameter $\theta(t) = -0.07t + 2t$ and cubic forcing parameter $\theta(t) = 0.0001(t - 25)^3 - 0.001t^2 + 3$, observing data for both position and velocity, along with the corresponding predicted mass-spring system states for position (middle) and velocity (right). In each approximation plot, $\theta_{\text{est}}(t)$ is shown in solid red and the true $\theta(t)$ is shown in dashed black. In each prediction plot, the state prediction using $\theta_{\text{est}}(t)$ is shown in red and the true model solution is shown in solid black.

Coefficient	Linear Forcing Parameter	Cubic Forcing Parameter
c_1	-0.2596 ± 1.8563	0.6518 ± 1.7268
c_2	0.6511 ± 1.8842	0.3946 ± 1.9433
c_3	1.3101 ± 4.2451	1.0047 ± 4.2206
c_4	2.1833 ± 4.3062	1.7988 ± 4.3596
c_5	-0.0451 ± 5.5032	1.8021 ± 5.4017
c_6	0.1796 ± 5.3475	-0.3192 ± 5.6353
c_7	1.9984 ± 6.1184	3.4025 ± 6.1732
c_8	-1.4737 ± 4.8591	-0.8341 ± 4.8626
RMSE	0.2069	0.2542

Table 3: Final coefficient estimates (mean \pm 2 standard deviations) and RMSE values to four decimal places when using model (15) to estimate the linear forcing parameter $\theta(t) = -0.07t + 2t$ and cubic forcing parameter $\theta(t) = 0.0001(t - 25)^3 - 0.001t^2 + 3$, observing data for both position and velocity.

4 Discussion and Conclusions

In this work, we proposed a Fourier series-based approximation method for estimating time-varying parameters in deterministic dynamical systems. More specifically, we represented the time-varying parameter $\theta(t)$ as a linear combination of sine and cosine functions with differing frequencies and estimated the unknown coefficients using ensemble Kalman filtering. The posterior EnKF mean estimates were then utilized in computing an approximation $\theta_{\text{est}}(t)$ of the time-varying parameter. With examples using a forced mass-spring system, we demonstrated the capability of this approach in approximating a periodic forcing parameter in cases when the period was assumed to be known and unknown, as well as polynomial forcing parameters that were not assumed to be periodic over the time interval of observed data.

Considering first a two-term approximation model with sine and cosine terms having the same frequency as the true periodic parameter $\theta(t) = \sin(t)$, we validated the approach and compared the accuracy of results when having partial vs. full system observations. Results in Figure 3 and Table 1 demonstrate, perhaps unsurprisingly, that observing both system components results in a more accurate approximation than observing only position or velocity. However, when partially observing the system, the resulting approximations still capture the overall behavior of $\theta(t)$ while under-estimating the amplitude of the sine curve. Further, observing only velocity results in a more accurate approximation than observing only position, which follows reasonably from $\theta(t)$ appearing in the equation for velocity in (9) and the cross-correlation information used in computing the Kalman gain; see, e.g., [17].

To accommodate cases when the period of $\theta(t)$ is unknown, we expanded the approximation models to include more terms with differing frequencies with the goal of determining coefficient values in the linear combination that well represent the underlying time-varying parameter. In particular, we utilized the low, high, and mixed frequency models given in (12), (13), and (14) to approximate $\theta(t) = \sin(t)$. Results in Figure 4 and Table 2 show that, while the estimated coefficient corresponding to the $\sin(t)$ term was the largest in each case (and generally close to 1), even relatively small nonzero contributions from terms with differing frequencies induce error in the resulting approximation. These results highlight the importance of choosing terms with appropriate frequencies in the time-varying parameter approximation model.

We then utilized an approximation model with lower frequency terms to estimate polynomial forcing parameters that were not periodic over the time interval of observed data. The results in Figure 5 and Table 3 show that using the lower frequency model in (15) provides a reasonable approximation for both the linear and cubic forcing parameters considered, capturing the overall trend of the time-varying parameter in each case. Note that while some of the coefficient estimates reported in Table 3 for the polynomial forcing parameters have relatively wider uncertainty bounds than in the previous numerical experiments, particularly for the terms with the smaller frequencies, the EnKF mean estimates result in time-varying parameter approximations that well represent the overall behavior of the true parameters. Further, even with some error, the time-varying parameter approximations can be utilized to make reasonable predictions of the mass-spring model states, as shown in Figure 5.

The Fourier Series-based approximation method proposed in this work yields promising results for estimating time-varying parameters in deterministic dynamical systems. Open questions remain, including how to select an appropriate number of sine and cosine terms in the approximation models and how to choose appropriate angular frequencies ω_i for those terms a priori. Future work includes performing a comparison between the Fourier series-based approximation models and linear approximation models using, e.g., radial basis functions and polynomial basis functions, as well as development of a systematic approach for selecting the terms in the approximation model.

Acknowledgments

This work was supported by the National Science Foundation under grant number NSF/DMS-1819203.

CRediT Authorship Contribution Statement

Anna Fitzpatrick: Formal analysis, Investigation, Methodology, Software, Validation, Visualization, Writing. **Molly Folino:** Formal analysis, Investigation, Methodology, Software, Validation, Visualization, Writing. **Andrea Arnold:** Conceptualization, Formal analysis, Funding acquisition, Methodology, Software, Supervision, Validation, Visualization, Writing.

Declaration of Competing Interest

The authors declare that they have no known competing financial interests or personal relationships that could have appeared to influence the work reported in this paper.

References

- [1] A. Arnold and A. L. Lloyd. An approach to periodic, time-varying parameter estimation using nonlinear filtering. *Inverse Problems*, 34:105005, 2018.
- [2] K. Campbell, L. Staugler, and A. Arnold. Estimating time-varying applied current in the Hodgkin-Huxley model. *Applied Sciences*, 10(2):550, 2020.
- [3] G. Kenne, T. Ahmed-Ali, F. Lamnabhi-Lagarrigue, and A. Arzande. Nonlinear systems time-varying parameter estimation: Application to induction motors. *Electric Power Systems Research*, 78:1881–1888, 2008.
- [4] N. Zhou, Z. Huang, Y. Li, and G. Welch. Local sequential ensemble Kalman filter for simultaneously tracking states and parameters. In *2012 North American Power Symposium (NAPS)*, Champaign, IL, USA, 2012. IEEE.
- [5] G. Konidaris, S. Osentoski, and P. Thomas. Value function approximation in reinforcement learning using the Fourier basis. In *Proceedings of the Twenty-Fifth AAAI Conference on Artificial Intelligence*, pages 380–385, 2011.
- [6] S. Liuzzo, R. Marino, and P. Tomei. Adaptive learning control of nonlinear systems by output error feedback. *IEEE Transactions on Automatic Control*, 52(7):1232–1248, 2007.
- [7] W. Chen, W. Li, and Q. Miao. Backstepping control for periodically time-varying systems using high-order neural network and Fourier series expansion. *ISA Transactions*, 49:283–292, 2010.
- [8] C.-L. Zhang and J.-M. Li. Hybrid function projective synchronization of chaotic systems with uncertain time-varying parameters via Fourier series expansion. *International Journal of Automation and Computing*, 9:388–394, 2012.
- [9] A. Arnold. Using Monte Carlo particle methods to estimate and quantify uncertainty in periodic parameters. In *Advances in Mathematical Sciences*, pages 213–226. Springer, 2020.

- [10] H. U. Voss, J. Timmer, and J. Kurths. Nonlinear dynamical system identification from uncertain and indirect measurements. *International Journal of Bifurcation and Chaos*, 14:1905–1933, 2004.
- [11] X. Bian, X. R. Li, H. Chen, D. Gan, and J. Qiu. Joint estimation of state and parameter with synchrophasors – Part II: parameter tracking. *IEEE Transactions on Power Systems*, 26:1209–1220, 2011.
- [12] M. Feng, P. Liu, S. Guo, L. Shi, C. Deng, and B. Ming. Deriving adaptive operating rules of hydropower reservoirs using time-varying parameters generated by the EnKF. *Water Resources Research*, 53:6885–6907, 2017.
- [13] A. Arnold. Exploring the effects of uncertainty in parameter tracking estimates for the time-varying external voltage parameter in the FitzHugh-Nagumo model. In *6th International Conference on Computational and Mathematical Biomedical Engineering*, pages 512–515, 2019.
- [14] G. Evensen. Sequential data assimilation with a nonlinear quasi-geostrophic model using Monte Carlo methods to forecast error statistics. *Ocean Dynamics*, 99:10143–10162, 1994.
- [15] G. Burgers, P. J. van Leeuwen, and G. Evensen. Analysis scheme in the ensemble Kalman filter. *Monthly Weather Review*, 126:1719–1724, 1998.
- [16] G. Evensen. The ensemble Kalman filter for combined state and parameter estimation. *IEEE Control Systems Magazine*, 29:83–104, 2009.
- [17] A. Arnold, D. Calvetti, and E. Somersalo. Parameter estimation for stiff deterministic dynamical systems via ensemble Kalman filter. *Inverse Problems*, 30:105008, 2014.
- [18] R. K. Nagle, E. B. Saff, and A. D. Snider. *Fundamentals of Differential Equations and Boundary Value Problems*. Pearson, 6 edition, 2011.